


# Myeloid differentiation factor-2 activates monocytes in patients with dilated cardiomyopathy

Rico Feldtmann<sup>1,2</sup>  | Andreas Kümmel<sup>1,2</sup> | Bishwas Chamling<sup>1,2</sup> |  
 Anne Strohbach<sup>1,2</sup> | Kristin Lehnert<sup>1,2</sup> | Stefan Gross<sup>1,2</sup> | Lisa Loerzer<sup>1,2</sup> |  
 Alexander Riad<sup>3</sup> | Diana Lindner<sup>4,5</sup> | Dirk Westermann<sup>4,5</sup> | Jens Fielitz<sup>1,2</sup> |  
 Marcus Dörr<sup>1,2</sup> | Stephan B. Felix<sup>1,2</sup>

<sup>1</sup>Department of Internal Medicine B, Cardiology, University Medicine Greifswald, Greifswald, Germany

<sup>2</sup>DZHK (German Centre for Cardiovascular Research), Partner Site Greifswald, Greifswald, Germany

<sup>3</sup>DRK-Krankenhaus Teterow gGMBH, Internal Medicine, Teterow, Germany

<sup>4</sup>Department of Cardiology, University Heart and Vascular Center, Hamburg, Germany

<sup>5</sup>DZHK (German Centre for Cardiovascular Research), Partner Site Hamburg/Kiel/Lübeck, Hamburg, Germany

## Correspondence

Stephan B. Felix, University Medicine Greifswald, Department of Cardiology and Internal Medicine B, Ferdinand-Sauerbruch-Straße, 17475 Greifswald, Germany.

Email: [stephan.felix@med.uni-greifswald.de](mailto:stephan.felix@med.uni-greifswald.de)

## Funding information

Deutsche Forschungsgemeinschaft, Grant/Award Number: FI 965/5-2; Deutsches Zentrum für Herz-Kreislaufforschung, Grant/Award Numbers: 81X2400109, 81Z5400153; European Regional Development Fund (EFRE), the German Technologie-Beratungs-Institut (TBI), Grant/Award Number: TBI-V-1-025-VBW-010

## Abstract

Plasma levels of myeloid differentiation factor-2 (MD-2), a co-receptor of toll-like-receptor 4 (TLR4), independently predict mortality in patients with dilated cardiomyopathy (DCM). We tested whether monocyte activation by MD-2 contributes to immune activation and inflammatory status in DCM patients. We found increased MD-2 plasma levels in 25 patients with recent-onset DCM ( $1250 \pm 80.7$  ng/ml) compared to 25 age- and gender-matched healthy controls ( $793.4 \pm 52.0$  ng/ml;  $p < 0.001$ ). Monocytes isolated from DCM patients showed a higher expression ( $141.7 \pm 12.4\%$ ;  $p = 0.006$  vs. controls) of the MD-2 encoding gene, *LY96* and an increased NF- $\kappa$ B-activation. Further, the TLR4-activator lipopolysaccharide (LPS) caused a higher increase in interleukin (IL)-6 in monocytes from DCM patients compared to controls (mean fluorescence intensity:  $938.7 \pm 151.0$  vs.  $466.9 \pm 51.1$ ;  $p = 0.005$ ). MD-2 increased IL-6 secretion in a TLR4/NF- $\kappa$ B-dependent manner in monocyte-like THP-1-cells as demonstrated by TLR4-siRNA and NF- $\kappa$ B-inhibition. Since endothelial cells (ECs) are responsible for recruiting monocytes to the site of inflammation, ECs were treated with MD-2 leading to an activation of Akt and increased secretion of monocyte-chemoattractant-protein-1 (MCP-1). Activation of ECs by MD-2 was accompanied by an increased

**Abbreviations:** CD, cluster of differentiation; DAMPs, damage-associated molecular patterns; DCM, dilated cardiomyopathy; HUVEC, human umbilical vein endothelial cells; IL, interleukin; LAV, left atrial volume; LBP, lipopolysaccharide-binding protein; LPS, lipopolysaccharide; LVEDD, left ventricular end-diastolic diameter; LVEF, left ventricular ejection fraction; LVM, left ventricular mass; MD-2, myeloid differentiation factor-2; MFI, mean fluorescence intensity; MyD88, myeloid differentiation factor 88; NF- $\kappa$ B, nuclear factor 'kappa-light-chain-enhancer' of activated B cells; NT-proBNP, N-terminal pro-B-type natriuretic peptide; PBMCs, peripheral blood mononuclear cells; TLR4, toll-like receptor 4.

This is an open access article under the terms of the [Creative Commons Attribution-NonCommercial-NoDerivs](https://creativecommons.org/licenses/by-nc-nd/4.0/) License, which permits use and distribution in any medium, provided the original work is properly cited, the use is non-commercial and no modifications or adaptations are made.

© 2022 The Authors. *Immunology* published by John Wiley & Sons Ltd.

expression of the adhesion molecules *CD54*, *CD106* and *CD62E*, resulting in an increased monocyte recruitment, which was attenuated by CD54 inhibition. In addition, in murine WT but not *LY96-KO* bone marrow-derived macrophages LPS increased the amount of CD54 and CD49d/CD29. MD-2 facilitates a pro-inflammatory status of monocytes and EC-mediated monocyte recruitment via TLR4/NF- $\kappa$ B. Elevated MD-2 plasma levels are possibly involved in monocyte-related inflammation-promoting disease progression in DCM. Our results suggest that MD-2 contributes to increasing monocytic inflammatory activity and triggers the recruitment of monocytes to ECs in DCM.

#### KEYWORDS

dilated cardiomyopathy, Interleukin-6, monocytes, myeloid differentiation factor 2, toll-like receptor 4

## INTRODUCTION

Dilated cardiomyopathy (DCM) is characterized by systolic dysfunction and dilatation of the left or both ventricles. Besides various risk factors, innate immunity involving monocytes and macrophages plays a role in disease development and progression [1]. Recent clinical and experimental evidence suggests that toll-like receptor 4 (TLR4) activation and the resulting inflammatory response in the myocardium are pivotal for worsening of cardiac function [2, 3].

TLR4 is an important innate immune receptor expressed by various cell types mediating inflammation [1, 4]. Proper receptor activation is mediated by lipopolysaccharide (LPS)-binding protein (LBP), cluster of differentiation 14 (CD14) and myeloid differentiation factor-2 (MD-2) [5, 6]. LBP and CD14 transport LPS to the membrane-bound TLR4 receptor, where LPS is transmitted to MD-2 [3]. In the absence of MD-2, LPS has little to no effect on TLR4 activation [6–8]. The dimerization of TLR4/LPS/MD-2 complexes induces myeloid differentiation factor 88 (MyD88)-dependent and MyD88-independent pathways [5]. Both activate transcription factors such as activator protein-1, nuclear factor ‘kappa-light-chain-enhancer’ of activated B cells (NF- $\kappa$ B) and interferon regulatory factors culminating in inflammatory responses [9, 10]. Besides LPS, which is part of the outer membrane of gram-negative bacteria, so-called damage-associated molecular patterns (DAMPs) are also able to activate TLR4 [11].

MD-2 is a 20–25 kDa protein that occurs either as plasma protein or is membrane bound and co-localized with TLR4 [12]. Recently, we reported that elevated MD-2 plasma levels independently predict all-cause mortality in DCM patients [13]. We also showed that the combined measurement of NT-proBNP and MD-2 in plasma significantly improved mortality risk prediction in DCM patients compared to NT-proBNP alone [13]. Furthermore, we demonstrated that MD-2 mediates

negative inotropic effects on isolated cardiomyocytes *in vitro* [13]. Inflammation plays an important role in the pathophysiology of heart failure. Inflammatory cytokine levels are associated with the prognosis of heart failure patients and monocytes are a major source of inflammatory cytokines [14]. Furthermore, it could be shown that soluble cellular adhesion molecules are elevated in heart failure patients reflecting enhanced cell surface expression of these molecules, which is crucial to monocyte recruitment and homing [14]. Here, we tested the hypothesis that MD-2 is involved in the activation and recruitment of monocytes, thereby enhancing inflammatory responses in DCM.

## METHODS

### Study design

DCM patients were retrospectively examined in a case-control design focusing on the inflammatory activity of circulating monocytes in relation to detected MD-2 plasma levels. The goal of the study was to determine whether DCM patients had elevated MD-2 plasma levels compared to healthy subjects. Furthermore, we tested the hypothesis that elevated MD-2 plasma levels are associated with the inflammatory activity of circulating monocytes as defined by the degree of phosphorylation of NF- $\kappa$ B and IL-6 secretion.

### Study population

Between March 2015 and May 2019, we included 25 patients with recent-onset DCM. Recent-onset DCM was defined as a symptom history of less than 6 months [15], a reduced left ventricular ejection fraction (LVEF



<40%) and an increased left ventricular end-diastolic diameter according to HENRY score (LVEDD<sup>acc.</sup> to HENRY > 117%) [16]. Exclusion criteria were primary valvular diseases ( $\geq$  second degree), acute myocarditis, active infectious diseases, pulmonary diseases, cancer, chronic alcoholism and heart failure of other origins. All patients underwent a detailed medical interview, physical examination, laboratory tests, echocardiography and coronary angiography and received standard heart failure medication according to the guidelines of the European Society of Cardiology (ESC) [17]. Twenty-five age- and gender-matched healthy individuals were recruited as controls by the local blood donation centre of the University Medicine Greifswald. All participants gave written informed consent prior to inclusion. The investigation conforms with the principles outlined in the Declaration of Helsinki and its amendments [18]. The patient registries and the recruitment of the healthy controls were approved by the Ethics Committee of the University Medicine Greifswald, Germany (internal reg. Numbers BB013/15, BB012/18 and BB074/15).

## Statistical analysis

Data are expressed as mean  $\pm$  standard error of the mean (SEM) of at least three independent experiments. For statistical analysis, GraphPad Prism 5 (GraphPad Software, Inc., Jolla, CA, USA) was used. Baseline characteristics of patients and controls were compared using either chi-square test for categorical variables or the two-tailed t-test for continuous variables. Overall statistical differences in experimental data sets were calculated by using a one-way ANOVA, followed by calculating differences between groups using a two-tailed t-test. Statistical difference of relative changes was calculated by using a one-sample t-test. Pearson correlation was used to analyse the pairwise correlation amongst parameters. Unless otherwise stated,  $p < 0.05$  was considered statistically significant for all data analysis.

Detailed information on chemicals used and on methods of two-dimensional transthoracic echocardiography, preparation of peripheral blood monocytes, LEGENDplex™ multi-analyte flow assay kit, flow cytometry in general as well as quantification of monocyte subpopulations and intracellular IL-6, cell culture, RNA isolation, cDNA synthesis, quantitative real-time PCR, TLR4 knockdown assay, NF- $\kappa$ B inhibition in THP-1 cells, protein isolation and Western blot, ELISA and quantification of monocyte adhesion and CD54 attenuation and LY96 deficient bone marrow-derived macrophages are available as Supplementary methods.

## RESULTS

### Baseline characteristics

We included 25 DCM patients with recent-onset DCM ( $n = 10$  females, mean age  $55.2 \pm 14.5$  years). Twenty-five age- and gender-matched healthy individuals ( $n = 10$  females, mean age  $52.7 \pm 4.9$  years) served as controls. Baseline characteristics are shown in Table 1.

### Elevated MD-2 levels in monocytes of DCM patients are accompanied by enhanced NF- $\kappa$ B phosphorylation

Since changes of monocyte quantities have been described in heart failure of different origins and monocytes are a possible source of MD-2, monocyte subpopulations were characterized and quantified in the blood of DCM and control patients using multi-colour flow cytometry. According to their CD14 and CD16 expressions, monocytes were classified as classical (CD14<sup>+</sup>CD16<sup>-</sup>), intermediate (CD14<sup>+</sup>CD16<sup>+</sup>) and non-classical (CD14<sup>-</sup>CD16<sup>+</sup>) (Figure 1a). No differences in the abundance of classical (DCM vs. control;  $0.360 \pm 0.038$  Gpt/l vs.  $0.383 \pm 0.037$  Gpt/l;  $p = 0.67$ ), intermediate (DCM vs. control;  $0.041 \pm 0.005$  Gpt/l vs.  $0.043 \pm 0.007$  Gpt/l;  $p = 0.79$ ) and non-classical monocytes (DCM vs. control;  $0.033 \pm 0.007$  GPT/l vs.  $0.037 \pm 0.006$  Gpt/l;  $p = 0.74$ ) were detected between DCM patients and controls (Figure 1b). To investigate whether monocytes synthesize MD-2, we determined MD-2 plasma levels and LY96 mRNA expression in monocytes isolated from DCM patients and healthy controls. The MD-2 protein amount was significantly increased in the plasma of DCM patients ( $1250 \pm 80.7$  ng/ml) compared to healthy controls ( $793.4 \pm 52.0$  ng/ml;  $p < 0.001$ ; Figure 1c). Additionally, LY96 expression was significantly increased in monocytes of DCM patients ( $141.7 \pm 12.4\%$ ;  $p = 0.006$ ) compared to healthy individuals ( $100.0 \pm 7.8\%$ ; Figure 1d). Activation of the TLR4/MD-2 system mediates inflammation via NF- $\kappa$ B-signalling [19]. Indeed, Western blot analysis of proteins isolated from monocytes revealed an activation of NF- $\kappa$ B-signalling in DCM patients compared to healthy individuals (Figure 1e,f and Figure S1). Specifically, we found a significantly enhanced NF- $\kappa$ B p65 phosphorylation at Ser536 resulting in an increased phospho-NF- $\kappa$ B/NF- $\kappa$ B-ratio in monocytes from DCM patients compared to healthy controls ( $1.4 \pm 0.2$  vs.  $0.8 \pm 0.1$ ;  $p = 0.004$ ). Since MD-2 mediates TLR4 signalling that converges onto NF- $\kappa$ B, we hypothesized that increased MD-2 levels and NF- $\kappa$ B activity in monocytes of DCM patients reflect an increased TLR4-signalling. In summary, these data indicate that monocyte activity rather than the amount

**TABLE 1** Baseline characteristics of patients with recent-onset dilated cardiomyopathy at first hospital admission and healthy individuals

Parameter	DCM [ <i>n</i> = 25]	Healthy individuals [ <i>n</i> = 25]	<i>p</i> -value
Age [years]	57.4 ± 2.9	52.3 ± 0.1	
Female [ <i>N</i> (%)]	10 (40.0)	10 (40.0)	
Disease duration [months]	1.1 ± 0.2		
Echocardiography			
LVEF [%]	26.5 ± 1.3		
LVEDD Henry [%]	133.6 ± 2.1		
LVESD [mm]	58.1 ± 1.6		
IVSD [mm]	10.5 ± 0.4		
PWD [mm]	10.3 ± 0.5		
LVEDV [ml]	204.5 ± 22.1		
LVESV [ml]	148.4 ± 18.0		
LVM [g]	306.5 ± 15.6		
LVMi [g/m <sup>2</sup> ]	149.7 ± 6.2		
LA area (4 chamber view) [cm <sup>2</sup> ]	28.3 ± 1.4		
LA area (2 chamber view) [cm <sup>2</sup> ]	30.9 ± 1.3		
LA length [cm]	6.8 ± 0.2		
LA volume [ml]	116.6 ± 7.8		
LAVI [ml/m <sup>2</sup> ]	57.7 ± 4.1		
E [cm/s]	88.5 ± 5.9		
E/E'	13.6 ± 1.2		
TAPSE [mm]	17.6 ± 0.9		
Routine diagnostics and biochemical analysis			
Mitral valve insufficiency (< grade 2) [ <i>N</i> (%)]	25 (100)		
NT-proBNP [pg/ml]	2611 ± 536	48 ± 10	<0.001
hs CRP [mg/ml]	13.5 ± 4.4	2.2 ± 0.8	0.015
IL-6 [pg/ml]	26.5 ± 7.4	2.7 ± 0.4	0.003
MCP-1 [pg/ml]	271.1 ± 28.8	182.8 ± 15.7	0.011
eGFR (CKDI-EPI) [ml/min/1.73 m <sup>2</sup> ]	82.4 ± 3.1		
Leucocyte count [Gpt/l]	7.6 ± 0.5	6.7 ± 0.3	0.115
Haematocrit	0.44 ± 0.01	0.42 ± 0.01	0.050
NYHA classification			
NYHA I [ <i>N</i> (%)]	3 (12)		
NYHA II [ <i>N</i> (%)]	8 (32)		
NYHA III [ <i>N</i> (%)]	7 (28)		
NYHA IV [ <i>N</i> (%)]	7 (28)		
Cardiovascular risk factors			
Body mass index [kg/m <sup>2</sup> ]	30.2 ± 1.2		
Systolic blood pressure [mmHg]	118.6 ± 3.3		
Diastolic blood pressure [mmHg]	76.9 ± 2.6		
Heart rate [bpm]	78 ± 2.8		
Smoking [ <i>N</i> (%)]	15 (60)		
Diabetes mellitus [ <i>N</i> (%)]	2 (8)		

(Continues)



TABLE 1 (Continued)

Parameter	DCM [ <i>n</i> = 25]	Healthy individuals [ <i>n</i> = 25]	<i>p</i> -value
Medication at hospital release			
Beta blockers [ <i>N</i> (%)]	25 (100)		
ACE inhibitors [ <i>N</i> (%)]	18 (72)		
AT1 antagonists [ <i>N</i> (%)]	7 (28)		
Aldosterone antagonists [ <i>N</i> (%)]	24 (96)		
Statins	8 (32)		
Pacemaker devices [ <i>N</i> (%)]	0 (0)		
ICD devices [ <i>N</i> (%)]	2 (8)		

Note: Statistical analyses were performed using chi-square test for categorical variables or unpaired, two-tailed t-test for continuous variables.

Abbreviations: ACE, angiotensin-converting enzyme; AT1, angiotensin-II-receptor-subtype-1; BNP, brain natriuretic peptide; CD3, cluster of differentiation 3; CD68, cluster of differentiation 68; E/E', left ventricular filling index, ratio of maximal mitral inflow velocity to maximal relaxation velocity of the myocardium; E, peak velocity of mitral inflow in early diastole; HHV, human herpes virus; hsCRP, high sensitivity C-reactive protein; ICD, implantable cardioverter defibrillator; IL-6, Interleukin 6; IVSD, interventricular septum at end diastole; LA, left atrial; LAVI, left atrial volume index; LVEDD, left ventricular end-diastolic diameter according to Henry formula  $LVEDD_{Henry} = [45.3 \times \text{body surface area } 0.3] - [0.03 \times \text{age}] - 7.2$ ; LVEDV, left ventricular end-diastolic volume; LVEF, left ventricular ejection fraction; LVESD, left ventricular end-systolic diameter; LVESV, left ventricular end-systolic volume; LVM, left ventricular mass according to Devereux; LVMI, LVM indexed by body surface area; MCP-1, monocyte-chemoattractant-protein-1; NT-proBNP, n-terminal pro-B-type natriuretic Peptide; NYHA, New York Heart Association; PVB-19, parvovirus B19; PWD, posterior wall thickness; TAPSE, tricuspid annular plane systolic excursion.

of monocytes in specific subpopulations, as determined by differential expression of surface markers, accounts for the increased inflammation status of DCM patients.

### MD-2 plasma levels are associated with accumulation of IL-6 and enhanced NF-κB-phosphorylation in monocytes of DCM patients

TLR4/MD-2 receptors are strongly expressed on monocytes. Via the TLR4/MD-2 receptor, endotoxins cause an inflammatory activation of monocytes. By performing Pearson correlation analyses, we investigated a potential correlation between MD-2 plasma levels and NF-κB-phosphorylation as well as LPS-induced IL-6 accumulation in monocytes. We found a direct correlation between MD-2 plasma levels with the pNF-κB p65/NF-κB p65 ratio ( $r^2 = 0.41$ ,  $p = 0.001$ ) (Figure 2a) and intracellular IL-6 ( $r^2 = 0.29$ ,  $p = 0.005$ ) (Figure 2b), respectively. These data suggested an increased TLR4/MD-2/NF-κB-signalling in monocytes from DCM patients. To investigate this hypothesis, we treated whole blood of DCM patients and healthy controls with LPS in order to activate cytokine secretion via TLR4/MD-2/NF-κB-signalling. Brefeldin A and Monensin were added to prevent the secretion of IL-6 from and increase its intracellular amounts in monocytes to enable subsequent quantification by multi-colour flow cytometry. LPS-induced IL-6 accumulation was significantly increased in primary CD14<sup>+</sup> monocytes of DCM patients as compared to healthy controls ( $938.7 \pm 151.0$  vs.  $466.9 \pm 51.1$ ;  $p = 0.005$ ) (Figure 2c). These data

indicate that the TLR4/MD-2/NF-κB-signalling pathway is activated in monocytes of DCM patients.

### MD-2 increases IL-6 expression and secretion via TLR4 and NF-κB in THP-1 cells

To examine whether MD-2 regulates IL-6 expression, we treated THP-1 cells with recombinant MD-2 protein and determined IL-6 expression. Treatment with 10 ng/ml LPS served as positive control. MD-2 concentration and duration of stimulation were assessed by analyses of dose-response and time-course experiments (Figure S5). According to these experiments, an MD-2 concentration of 5 μg/ml and treatment duration of 24 hours were most effective regarding IL-6 mRNA expression in comparison to vehicle-treated controls. A possible LPS contamination of recombinant MD-2 protein was excluded by using polymyxin B (Figure S3). To investigate if the MD-2-induced IL-6 mRNA expression and protein secretion were mediated by TLR4, we transfected THP-1 cells for 24 hours with TLR4 siRNA (TLR4-KD, 100 nM) or non-targeting scrambled siRNA (control, 100 nM) (Figure 3a). The siRNA knockdown efficiency is presented in Figure S6. Both LPS- and MD-2 treatments lead to a significant increase in IL-6 expression (LPS:  $14410 \pm 1087\%$ ;  $p < 0.001$ ; MD-2:  $271 \pm 23\%$ ;  $p < 0.001$ ) in THP-1 cells treated with a scrambled siRNA compared to vehicle-treated control cells. TLR4-KD significantly reduced LPS- and MD-2-induced IL-6 expression (LPS:  $7336 \pm 1172\%$  vs.  $14410 \pm 1087\%$ ;  $p = 0.001$ ; MD-2:  $180 \pm 8\%$



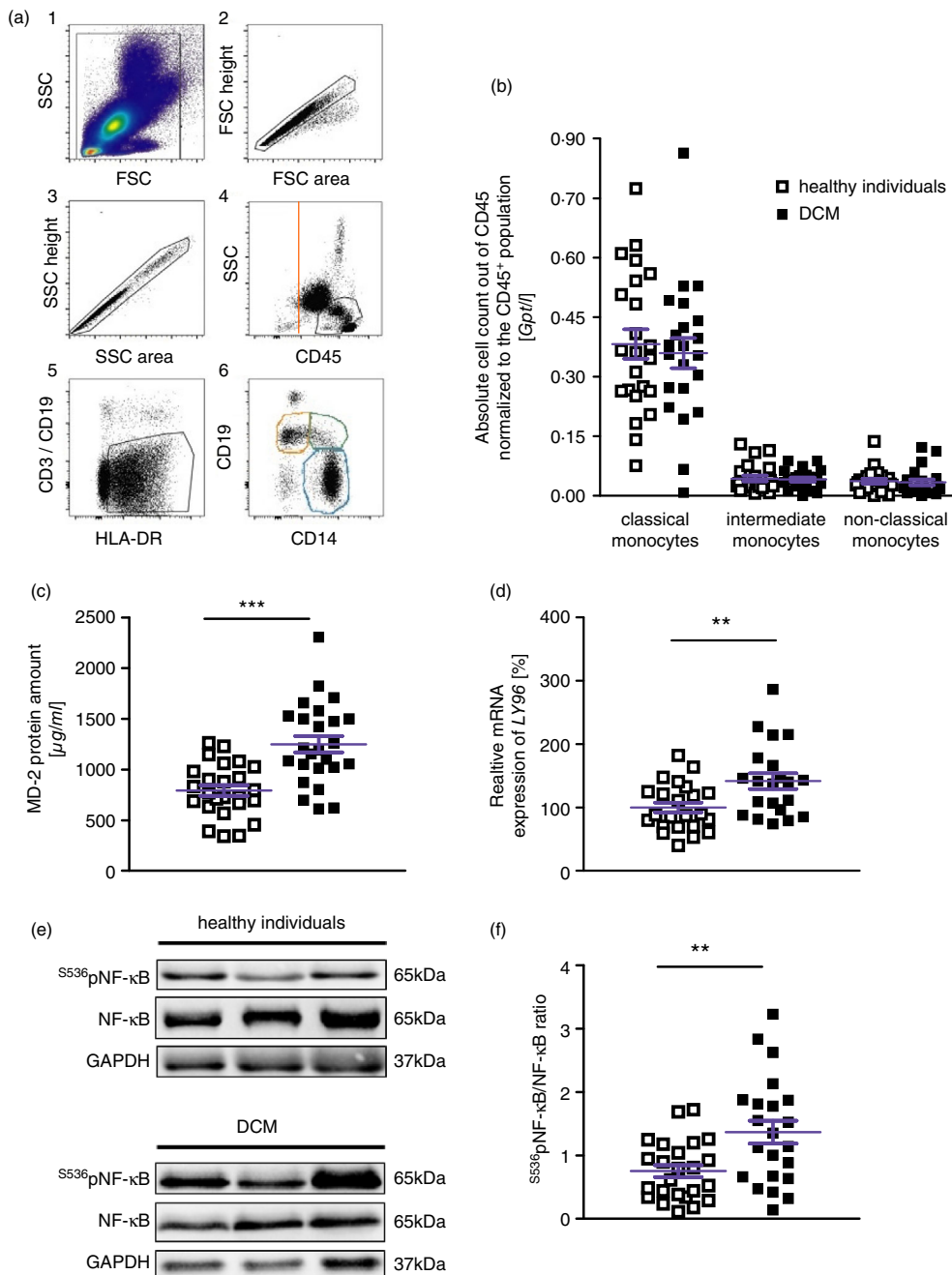


**FIGURE 1** MD-2 is elevated in monocytes of DCM patients. (a) Gating strategy for the identification of monocyte subpopulations. Image 1 shows the analysed cells in total based on forward (FSC) and side scatter (SSC). In images 2 and 3, cell aggregates were excluded. In image 4, the orange line shows the cut-off value for the definition and quantification of CD45 positive cells. The free-form gate was used to pre-separate monocytes from granulocytes and lymphocytes. In image 5, lymphocytes were excluded based on CD3 and CD19. HLA-DR was used to include monocytes. Image 6 shows the identification of the individual monocyte subpopulations (blue - classical monocytes, green - intermediate monocytes, orange - non-classical monocytes) using CD14 and CD16. (b) Monocyte subpopulations were identified by the expression of CD14 and CD16 via multi-colour flow cytometry. Absolute cell counts of classical CD14<sup>+</sup>CD16<sup>-</sup>, intermediate CD14<sup>+</sup>CD16<sup>+</sup> and non-classical CD14<sup>-</sup>CD16<sup>+</sup> monocytes were calculated using CD45 lymphocytes and the white blood cell count from routine diagnostics. Scatter plots show mean  $\pm$  SEM of 22 DCM patients and 23 healthy controls. (c) MD-2 was measured in plasma of DCM patients ( $n = 25$ ) and healthy controls ( $n = 25$ ) by ELISA. Scatter plots show mean  $\pm$  SEM of MD-2 protein. Statistical difference was determined using a two-tailed  $t$ -test with \*\*\* $p < 0.001$ . (d) LY96 expression from freshly isolated primary CD14<sup>+</sup> monocytes of DCM patients ( $n = 21$ ) was analysed by quantitative real-time PCR and compared to healthy controls ( $n = 23$ ). Scatter plots show mean  $\pm$  SEM. Statistical difference was determined using a two-tailed  $t$ -test with \*\* $p < 0.01$ . (e) The activation of NF- $\kappa$ B-signalling was quantified by Western blot analysis. A Western blot of protein lysates from monocytes isolated from three representative individuals per group (healthy individuals and DCM patients) is presented. NF- $\kappa$ B and pNF- $\kappa$ B were analysed separately and GAPDH served as a loading control. (f) Scatter plots show mean  $\pm$  SEM of the ratio of p65 NF- $\kappa$ B to total NF- $\kappa$ B normalized to GAPDH and a pooled sample for healthy individuals ( $n = 24$ ) and DCM patients ( $n = 22$ ). Statistical difference was determined using a two-tailed  $t$ -test with \*\* $p < 0.01$ .

vs.  $271 \pm 23\%$ ;  $p = 0.004$ ) and IL-6 secretion (LPS:  $46.14 \pm 1.91$  pg/ml vs.  $105.30 \pm 9.40$  pg/ml;  $p = 0.004$ ; MD-2:  $6.85 \pm 1.03$  pg/ml vs.  $10.65 \pm 0.22$  pg/ml;  $p = 0.023$ ) compared to scrambled siRNA treated controls (Figure 3b). As expected, LPS and MD-2 treatment of THP-1 cells, transfected with scrambled siRNA increased IL-6 secretion compared to vehicle-treated controls (LPS:  $105 \pm 9.40$  pg/ml vs.  $2.68 \pm 0.30$  pg/ml;  $p < 0.001$ ; MD-2:  $10.65 \pm 0.22$  pg/ml vs.  $2.68 \pm 0.30$  pg/ml;  $p < 0.001$ ).

In THP-1 cells, LPS-mediated TLR4/MD-2-activation leads to an increased phosphorylation of NF- $\kappa$ B. Thus, we examined whether MD-2 also activated NF- $\kappa$ B-signalling via TLR4 in the absence of LPS (Figure 3c,d). MD-2 ( $0.97 \pm 0.16$  vs.  $0.53 \pm 0.10$ ;  $p = 0.049$ ) and LPS ( $1.81 \pm 0.38$  vs.  $0.53 \pm 0.10$ ;  $p = 0.012$ ) increased NF- $\kappa$ B-phosphorylation compared to vehicle-treated controls. Importantly, NF- $\kappa$ B inhibition by BOT64-attenuated MD-2-induced IL-6 expression in a concentration-dependent manner (BOT64:  $5 \mu\text{M}$ :  $85.1 \pm 15.0\%$ ,  $p = 0.009$ ;  $10 \mu\text{M}$ :  $76.9 \pm 27.5\%$  vs.  $263.1 \pm 44.4\%$ ,  $p = 0.012$ ; Figure 3e). BOT64 ( $10 \mu\text{M}$ ) also inhibited LPS-induced IL-6 expression ( $824.7 \pm 376.5\%$  vs.  $16\,870 \pm 3682\%$ ;  $p = 0.005$ ; Figure 3e).

## MD-2 increases the adhesion of monocytes to endothelial cells

Since monocyte activation is closely linked to inflammatory EC activation and endothelial cells are responsible for the recruitment of monocytes, we investigated if MD-2 also affects the expression of adhesion molecules in HUVECs. In these cells, MD-2 increased the expression of the adhesion molecules *E-selectin* (*CD62E*;  $690.8 \pm 62.4\%$ ;  $p < 0.001$ ), *CD54* ( $233.6 \pm 20.0\%$ ;  $p = 0.001$ ) and *CD106* ( $894.3 \pm 233.2\%$ ;  $p = 0.019$ ) compared to vehicle-treated controls (Figure 4a). Likewise, LPS leads to an increased expression of *CD62E* ( $628.8 \pm 86.4\%$ ;  $p = 0.002$ ), *CD54* ( $636.0 \pm 175.8\%$ ;  $p = 0.028$ ) and *CD106* ( $740.3 \pm 101.0\%$ ;  $p = 0.001$ ). Additionally, MD-2 significantly increased *MCP-1* expression ( $231.7 \pm 39.5\%$ ;  $p = 0.029$ ) and protein content ( $8792 \pm 1213$  pg/ml;  $p = 0.006$ ) in HUVECs (Figure 4b, c). Likewise, LPS treatment increased *MCP-1* expression and absolute protein amount ( $327 \pm 70\%$ ;  $p = 0.032$  and  $17\,210 \pm 3063$  pg/ml;  $p = 0.002$ , respectively). Since it is known that IL-6-induced *MCP-1* expression is regulated by Akt phosphorylation at S473 [20], we investigated if MD-2-induced *MCP-1* expression was accompanied by Akt activation in HUVECs. HUVECs treated with MD-2 for 15 min showed a twofold increase of Akt phosphorylation at S473 (pAkt/Akt:  $0.73 \pm 0.02$  vs.  $0.36 \pm 0.07$ ;  $p = 0.008$ ), compared to vehicle-treated controls.

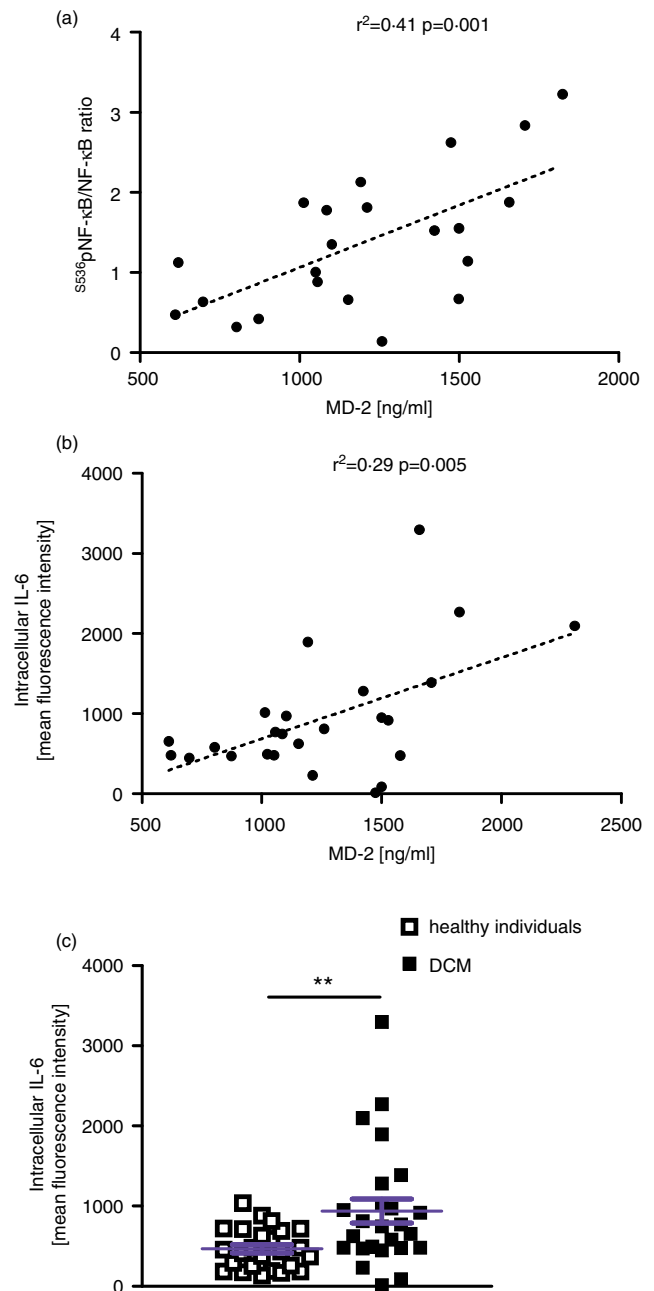


**FIGURE 2** MD-2 correlates to accumulated IL-6 and NF- $\kappa$ B in monocytes. Correlation of MD-2 plasma levels with NF- $\kappa$ B phosphorylation ( $n = 22$ ) (a) and intracellular accumulated IL-6 ( $n = 25$ ) (b) in monocytes of DCM patients. Each symbol represents data from one DCM patient. The data were analysed using a Pearson correlation test. Pearson correlation coefficients are displayed as  $r^2$  and a statistically significant difference is indicated by the  $p$ -value. Dashed lines visualize the direction of the correlation. (c) Intracellular IL-6 was accumulated in human monocytes after treatment of whole blood with 10 ng/ml LPS, 5  $\mu\text{g/ml}$  Brefeldin a and 2- $\mu\text{M}$  Monensin for 5 h. Blood samples from healthy individuals ( $n = 25$ ) and DCM patients ( $n = 25$ ) were analysed by flow cytometry. Monocytes were defined as  $\text{CD45}^+/\text{HLA-DR}^+/\text{CD14}^+$  and  $\text{CD3}^-/\text{CD19}^-$  cells. Scatter plots show mean  $\pm$  SEM of mean fluorescence intensity (MFI). Statistical difference was determined using a two-tailed  $t$ -test with  $**p < 0.01$ .

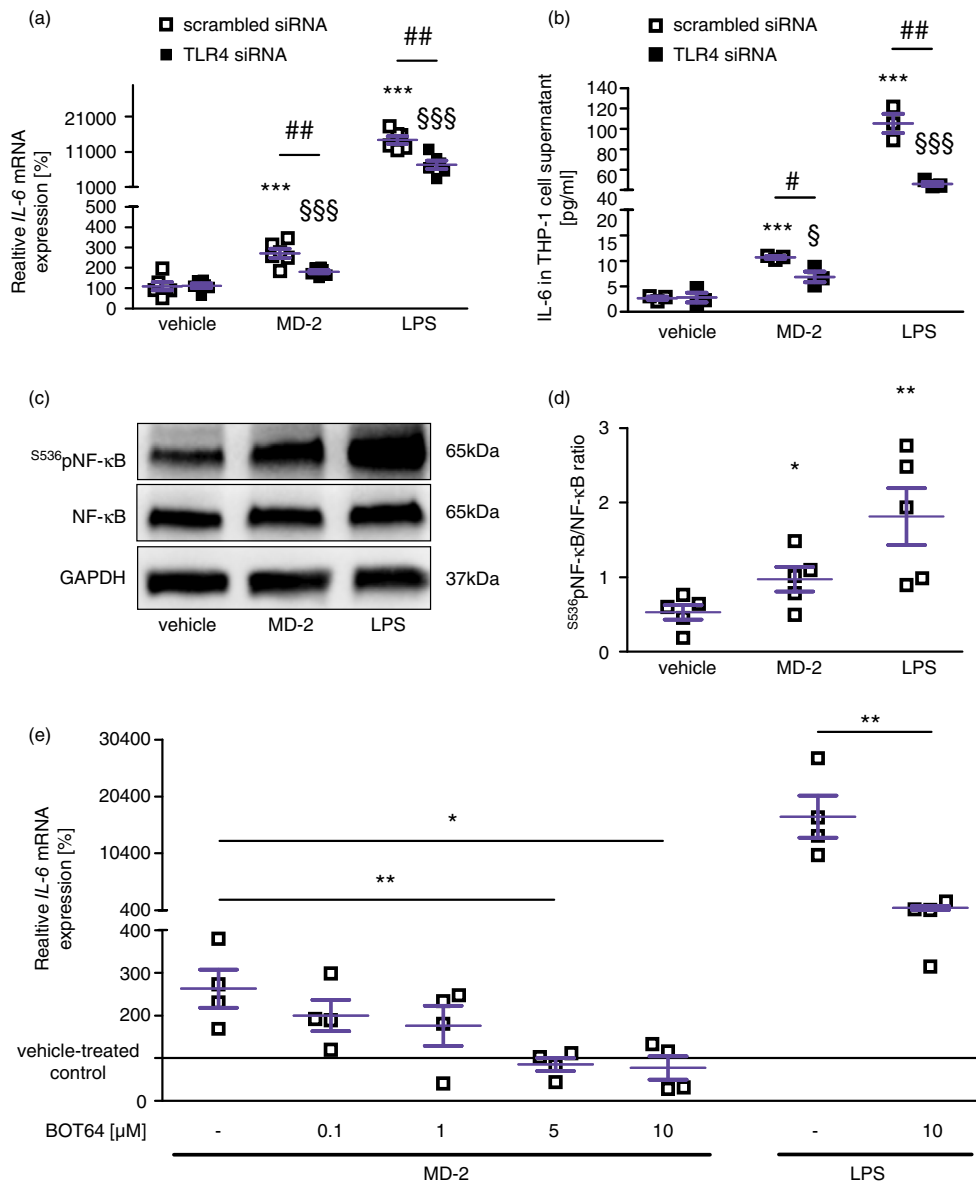


**FIGURE 3** MD-2 induces secretion of IL-6 via TLR4 and NF- $\kappa$ B in THP-1 cells. (a,b) Cells were transfected with 100 nM TLR4-siRNA or scrambled-siRNA for 24 h and then treated with MD-2 (5  $\mu$ g/ml) or LPS (10 ng/ml) for 24 h. (a) IL-6-mRNA was determined by quantitative real-time PCR. Results are given as scatter plots with mean  $\pm$  SEM of six independent experiments and are displayed relative to scrambled-siRNA vehicle-treated control. Overall statistical differences were determined by using a one-way ANOVA (six groups). Post hoc group-wise comparisons were done using two-tailed *t*-tests: Significant differences to scrambled-siRNA/TLR4-siRNA vehicle-treated control are shown as \*\*\**p* < 0.001/§§§*p* < 0.001. Changes within treatment groups are displayed as ##*p* < 0.01. (b) The IL-6 concentration in THP-1 supernatants from pre-treated cells was determined using ELISA. Results are given as scatter plots with mean  $\pm$  SEM of three independent experiments. Overall statistical differences were determined by using a one-way ANOVA (six groups). Post hoc group-wise comparisons were done using two-tailed *t*-tests: Significant differences to scrambled-siRNA/TLR4-siRNA vehicle-treated control are shown as \*\*\**p* < 0.001/§*p* < 0.05; §§§*p* < 0.001. Changes within treatment groups are displayed as #*p* < 0.05; ##*p* < 0.01. (c) A representative Western blot of assessed Ser<sup>536</sup>NF- $\kappa$ B-phosphorylation is presented. THP-1 cells were treated with 5  $\mu$ g/ml MD-2 or 10 ng/ml LPS for 20 min. (d) Scatter plots show mean  $\pm$  SEM of the pNF- $\kappa$ B/total-NF- $\kappa$ B-ratio normalized to GAPDH of five independent experiments. Overall statistical differences were determined by using a one-way ANOVA (three groups). Post hoc comparisons were done using two-tailed *t*-tests: Statistical differences to the vehicle-treated control are displayed as \**p* < 0.05. (e) Prior to MD-2/LPS treatment, cells were incubated for 2 h with BOT64. IL-6-expression was determined by quantitative real-time PCR. Results are given as scatter plots with mean  $\pm$  SEM of four independent experiments and are displayed relative to vehicle-treated control. Overall statistical differences were determined by using a one-way ANOVA (seven groups). Post hoc group-wise comparisons were done using two-tailed *t*-tests: Significant differences to the MD-2/LPS-BOT64 negative treatment groups are indicated as \**p* < 0.05; \*\**p* < 0.01.



Likewise, LPS caused a threefold increase in Akt phosphorylation at S473 compared to vehicle-treated controls (pAkt/Akt:  $1.07 \pm 0.13$  vs.  $0.36 \pm 0.07$ ;  $p = 0.010$ ) (Figure 4d,e). These data indicate that MD-2 not only activates monocytes but also activates endothelial cells.

Because MCP-1 mediates the recruitment of monocytes and their adhesion to ECs, we investigated the impact of MD-2 on the adhesion of freshly isolated

PBMCs from healthy volunteers. HUVECs were pre-treated with MD-2 or LPS for 48 hours and subsequently incubated with PBMCs for 20 minutes. Treatment with LPS served as a positive control. As shown in Figure 4f, MD-2 as well as LPS increased the adhesion of monocytes to HUVECs compared to vehicle-treated controls (MD-2:  $2.38 \pm 0.23$  vs.  $1.57 \pm 0.16$ ;  $p = 0.013$ ; LPS:  $3.23 \pm 0.17$  vs.  $1.57 \pm 0.16$ ;  $p < 0.001$ ). Since MD-2 increased the

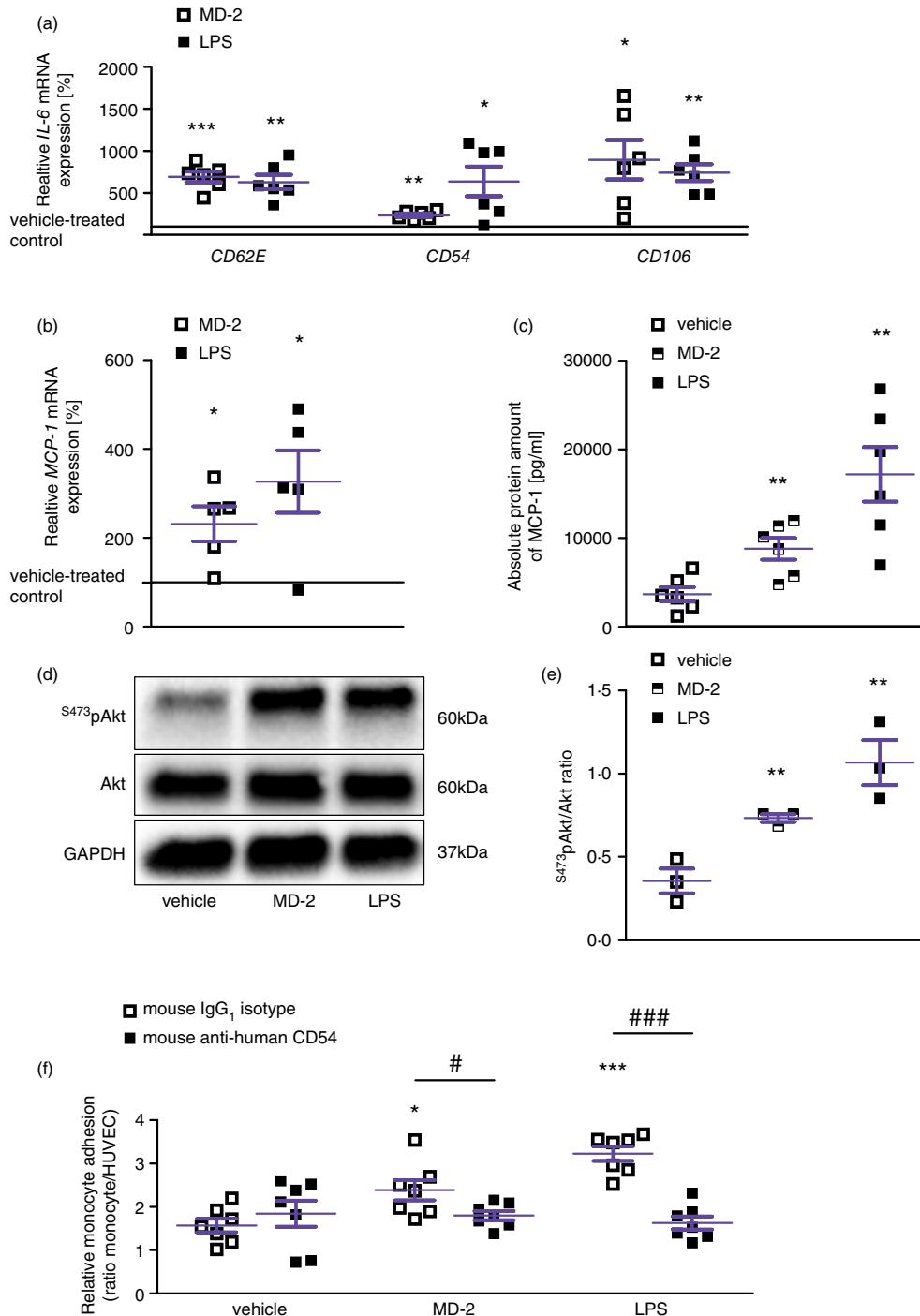


FIGURE 4 Legend on next page.

expression of the adhesion molecule *CD54* in ECs, we examined whether *CD54* contributes to MD-2-mediated monocyte adhesion onto HUVECs and whether blockage with an anti-*CD54* antibody attenuates this effect. Therefore, HUVECs were incubated for 30 minutes with a mouse anti-human *CD54* or a mouse IgG1 isotype antibody prior to the addition of PBMC. MD-2- and LPS-induced monocyte adhesion was diminished by *CD54* blockade (MD-2:  $1.80 \pm 0.11$  vs.  $2.38 \pm 0.23$ ;  $p = 0.042$ ; LPS:  $1.63 \pm 0.15$  vs.  $3.23 \pm 0.17$ ;  $p < 0.001$ ) when compared to treatment with an IgG1 isotype antibody. These data indicate that MD-2 facilitates monocyte to ECs adhesion and that this effect is mediated at least partially by *CD54*.

### Bone marrow-derived macrophages from *LY96* knockout mice are less LPS responsive

Once activated and adhered to the endothelium, monocytes differentiate into macrophages. We isolated BMDMs from *LY96*-KO mice using L929-conditioned media in order to characterize the involvement of MD-2 in LPS-dependent macrophage activation. C57BL6/N WT mice were used as controls. BMDMs were defined as F4/80 and MHC II positive cell population analysed by flow cytometry. After 7 days of *in vitro* cell culture, BMDMs were differentiated into macrophages (Figure S2). After differentiation, WT and *LY96*-KO macrophages were treated with increasing concentrations of LPS. Increasing amounts of LPS resulted in an increased expression of the adhesion molecules *CD54* and *CD49d/CD29* in macrophages of WT mice, which was significantly lower in macrophages from *LY96*-KO mice when compared to WT mice treated with 10 ng/ml LPS, (*CD54*:  $1318 \pm 534\%$

vs.  $4105 \pm 1129\%$ ;  $p = 0.0497$ ; *CD49d/CD29*:  $169 \pm 13\%$  vs.  $428 \pm 74\%$ ;  $p = 0.006$ ) (Figure 5a). *CD54* and *CD49d/CD29* protein contents were also reduced in *LY96*-KO compared to WT macrophages (*CD54*:  $0.66 \pm 0.09$  vs.  $1.50 \pm 0.25$ ;  $p = 0.012$ ; *CD49d/CD29*:  $0.75 \pm 0.16$  vs.  $1.44 \pm 0.20$ ;  $p = 0.024$ ) (Figure 5b,c). Finally, we examined the phosphorylation of NF- $\kappa$ B in LPS-treated *LY96*-KO macrophages as well (Figure 5d,e). NF- $\kappa$ B-phosphorylation of vehicle-treated and LPS-treated BMDMs of both genotypes revealed no significant differences for low concentration of LPS (1 ng/ml). Treatment with high concentrations of LPS (10 ng/ml), however, leads to a 2.5-fold increase in NF- $\kappa$ B-phosphorylation in macrophages from C57BL6/N WT mice (pNF- $\kappa$ B/NF- $\kappa$ B:  $1.42 \pm 0.28$  vs.  $0.58 \pm 0.15$ ;  $p = 0.042$ ), which was completely blunted in *LY96*-KO mice ( $0.84 \pm 0.19$  vs.  $0.69 \pm 0.11$ ;  $p = 0.550$ ).

### DISCUSSION

The innate immune system is primarily involved in the pathophysiology of heart failure by inducing systemic inflammation [14]. Recent clinical data suggest that TLR4 activation is involved in the worsening of cardiac function and two variants of toll-like receptor 4 (rs4986790, rs4986791) predict cardiac recovery in patients with recent-onset DCM [2]. Moreover, experimental studies indicate that innate immune receptors, innate immune signalling pathways and pro-inflammatory cytokines activated by these pathways contribute to LV remodelling in response to myocardial injury [1]. Monocytes are an important source of pro-inflammatory cytokines [14] and cytokine release is induced after activation of the TLR4/MD-2 complex [21]. Experimental data show that inflammation and cardiac

**FIGURE 4** MD-2 induces adhesion of monocytes to endothelial cells. (a) HUVECs were treated with LPS (10 ng/ml) or MD-2 (5  $\mu$ g/ml) for 24 h. Adhesion molecule mRNA expression was normalized to *GAPDH* and compared to a vehicle-treated control. Scatter plots show mean  $\pm$  SEM of six independent experiments. Statistical differences to the vehicle-treated control were determined using a one-sample *t*-test and are indicated with \* $p < 0.05$ ; \*\* $p < 0.01$ ; \*\*\* $p < 0.001$ . (b) HUVECs were treated for 24 h with MD-2 (5  $\mu$ g/ml) or LPS (10 ng/ml). *MCP-1* mRNA expression was normalized to *GAPDH* and compared to a vehicle-treated control. Scatter plots show mean  $\pm$  SEM of five independent experiments. Statistical difference to the vehicle-treated control was determined using a one-sample *t*-test and is indicated as \* $p < 0.05$ . (c) *MCP-1* protein abundance was determined in supernatants of MD-2- and LPS-treated HUVECs after 48 h. Scatter plots show mean  $\pm$  SEM of protein amounts of six independent experiments quantified by ELISA. Overall statistical differences were determined by using a one-way ANOVA (three groups). Post hoc statistical difference to the vehicle-treated control was determined using a two-tailed *t*-test and is displayed as \*\* $p < 0.01$ . (d) HUVECs were stimulated with MD-2 (5  $\mu$ g/ml) and LPS (10 ng/ml) for 15 min. A representative Western blot of assessed Ser<sup>473</sup>Akt phosphorylation is presented. (e) Scatter plots show mean  $\pm$  SEM of the pAkt/total-Akt ratio normalized to *GAPDH* of three independent experiments. Overall statistical differences were determined by using a one-way ANOVA (three groups). Post hoc statistical difference to the vehicle-treated control was determined using a two-tailed *t*-test and is displayed as \*\* $p < 0.01$ . (f) HUVECs were treated for 48 h and incubated with 1  $\mu$ g/ml of a mouse-anti-human *CD54* or an IgG1 isotype antibody for 30 min prior to PBMC incubation. Cells were analysed by flow cytometry. HUVECs were defined as  $CD31^+/CD45^-/CD14^-$ , monocytes as  $CD45^+/CD31^-/CD14^+$ . Scatter plots show mean  $\pm$  SEM of seven independent experiments. Overall statistical differences were determined by using a one-way ANOVA (six groups). Post hoc comparisons were done using two-tailed *t*-tests: Significant differences to a vehicle-treated isotype control are given as \* $p < 0.05$ ; \*\*\* $p < 0.001$ . Changes within treatment groups are displayed as # $p < 0.05$ ; ## $p < 0.01$ .

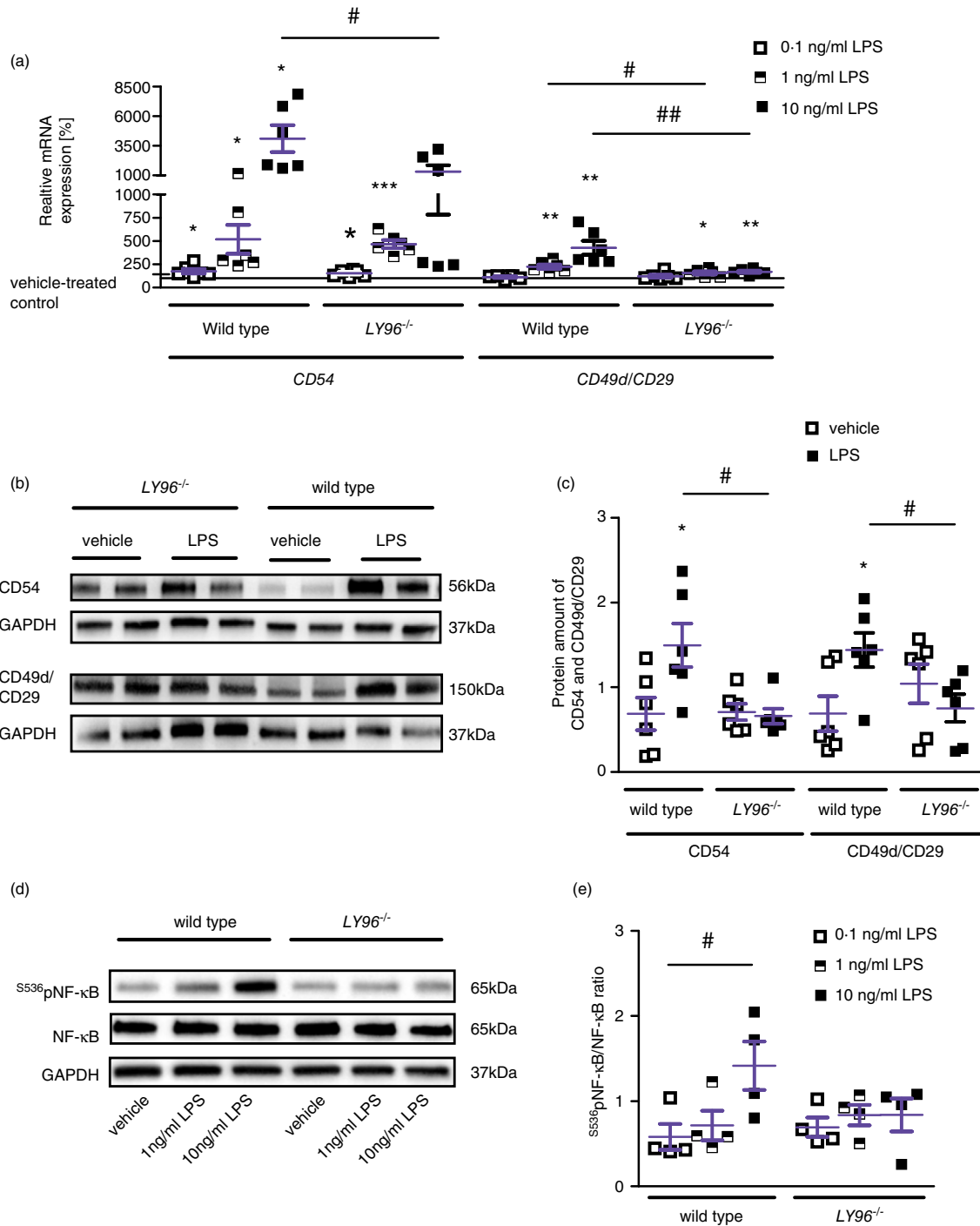


**FIGURE 5** Bone marrow-derived macrophages (BMDMs) from *MD-2* knockout mice are less responsive to LPS. BMDMs of C57BL/6N wild type and *MD-2* knockout mice were treated with LPS (0.1 ng/ml, 1 ng/ml and 10 ng/ml) for 24 h. (a) *CD54* and *CD49d/CD29* gene expressions were normalized to *GAPDH* and compared to a vehicle-treated control (black line). Scatter plots show mean  $\pm$  SEM of six independent experiments. Statistical differences to the vehicle-treated control were determined using a one-sample *t*-test and are indicated with \**p* < 0.05; \*\**p* < 0.01; \*\*\**p* < 0.001. For *CD54* and *CD49d/CD29*, the overall statistical differences were determined independently by using a one-way ANOVA (six groups each). Post hoc comparisons were done using two-tailed *t*-tests: Significant differences between groups are given as #*p* < 0.05; ##*p* < 0.01. (b) The protein amount of *CD54* and *CD49d/CD29* was assessed by Western blot analysis. A representative Western blot is presented. (c) Scatter plots show mean  $\pm$  SEM of six independent experiments. For *CD54* and *CD49d/CD29*, the overall statistical differences were determined independently by using a one-way ANOVA (four groups each). Post hoc comparisons were done using two-tailed *t*-tests: Significant difference to a vehicle-treated control is given as \**p* < 0.05. Significant differences between treatment groups are given as #*p* < 0.05. (d) BMDMs of C57BL/6N and *MD-2* knockout mice were treated with LPS (1 ng/ml and 10 ng/ml) for 10 min. A representative Western blot of assessed Ser536pNF-κB-phosphorylation is presented. (e) Scatter plots show mean  $\pm$  SEM of the ratio of p65 NF-κB (S536) to total NF-κB normalized to GAPDH of four independent experiments. Overall statistical differences were determined by using a one-way ANOVA (six groups). Post hoc comparisons were done using two-tailed *t*-tests: Significant difference to a vehicle-treated control is given as #*p* < 0.05.

remodelling induced by obesity-induced cardiomyopathy are attenuated in mice MD-2 knockout mice or after MD-2 inhibition [22]. In this context, it could be shown that arachidonic acid directly binds to MD-2, thereby reducing LPS-induced inflammation in macrophages and septic death in mice [23]. In addition to its membrane-bound form and co-localized with TLR4, MD-2 is also found as a soluble molecule in blood plasma [12]. Little is known about the MD-2 secretory pathway. Within its amino acid sequence, MD-2 possesses a consensus sequence for a secretory signal peptide and it has been described as a type II acute-phase protein secreted by hepatocytes in response to an acute-phase reaction [24]. Recent studies suggest a strong contribution of TLR4 signalling in systemic inflammatory diseases and report an involvement of MD-2 plasma levels in this context [12, 25]. Recently, we described elevated MD-2 plasma levels in patients with DCM indicating that MD-2 is a prognostic biomarker in DCM [13]. These findings emphasize the importance of innate immunity in disease progression. Thus, the present study aimed to elucidate the relation between elevated MD-2 plasma levels and TLR4-mediated signalling in recent-onset DCM patients.

Here, we report increased MD-2 plasma levels, which was accompanied by increased LPS-induced IL-6 production in monocytes of DCM patients. We identified NF- $\kappa$ B-dependent TLR4/MD-2-signalling to mediate this IL-6 production in blood monocytes and monocyte-like THP-1 cells. MD-2 induced the expression of adhesion molecules (*CD54*, *CD106* and *CD62E*) in ECs and facilitated monocyte adhesion via MCP-1, which was attenuated by blocking CD54. Finally, we demonstrated the relevance of MD-2 in macrophage adhesion molecule expression and activation via NF- $\kappa$ B in macrophages from *LY96*-KO mice. Based on the current literature [26, 27], we expected changes in the abundance of monocyte subpopulations in DCM patients due to the inflammatory potential of MD-2. However, we did not detect differences in cell counts of monocyte subpopulations in our cohort of patients with recent-onset DCM. These data are in contrast to other studies that showed that patients with acute ischaemic heart failure [26] or with chronic systolic heart failure due to predominantly ischaemic aetiology [27] exhibit significant changes in the distribution of their monocyte subsets. We assume that these different findings might be related to other causes of heart failure. Interestingly, increased *LY96* mRNA expression in monocytes from septic patients has been reported together with increased MD-2 plasma levels [12]. Here, we found elevated *LY96* mRNA expression in monocytes from DCM patients which was accompanied by elevated MD-2 plasma levels as well. Our data give a first hint that beside hepatocytes, monocytes could be an additional source of MD-2. Increased plasma MD-2 levels have been suggested to act as an acute-phase reactant [24]. In this context, our

data suggest that the strength of monocyte activation is more important than their number.

Monocytes produce IL-6 in response to TLR4 activation [28]. Inflammatory cytokines amongst them IL-6 may be involved in the development of various inflammatory cardiac pathologies such as heart failure and cardiomyopathies [29] and, hence, be used as biomarkers of heart failure [30]. An acute increase in IL-6 levels is described to be cardioprotective and antiviral [31], whereas during long-term IL-6 signalling, an anti-cardiac autoimmune reaction can occur, leading to autoimmune myocarditis and subsequently to DCM and heart failure [32]. Our patients with recent-onset DCM exhibited significantly elevated IL-6 plasma levels. Furthermore, LPS-stimulated monocytes of DCM patients showed an increased NF- $\kappa$ B-phosphorylation and accumulated significantly more IL-6 than LPS-stimulated monocytes of healthy controls. This LPS-induced IL-6 production of patients' monocytes significantly correlated with MD-2 plasma levels. We conclude that MD-2-mediated immune activation and systemic inflammation are associated with the activation state of monocytes rather than with the abundance of monocyte subsets. Based on our data, we suggest that inhibition of the TLR4/MD-2 complex holds therapeutic potential for patients with recent-onset DCM.

To examine the mechanism of MD-2-induced IL-6 secretion, we used monocyte-like THP-1 cells. In these cells, MD-2 increased the IL-6 mRNA expression and protein secretion, which was mediated by TLR4/NF- $\kappa$ B-signalling. MD-2-induced *IL-6* expression was independent of LPS and was reduced by TLR4-siRNA KD or treatment with the cell membrane permeable IKK2 inhibitor BOT64. MD-2 is well studied within the TLR4/MD-2 complex and is typically described as a co-receptor mandatory for antigen binding [33] rather than an activator of TLR4 signalling. In our study, MD-2-mediated TLR4 activation in THP-1 cells as well as IL-6 release occurred independently of LPS.

Besides circulating immune cells, ECs respond to inflammation resulting in enhanced expression of adhesion molecules, which mediate the adhesion of leucocytes [34]. We report that treatment with MD-2 increases endothelial MCP-1 gene and protein expression, which is a well-described chemoattractant for monocytes [35]. In addition, DCM patients with severe left ventricular dysfunction also show elevated *MCP-1* mRNA expression in EMBs compared to patients with moderate left ventricular dysfunction [36] assuming that MD-2 is involved in increased MCP-1 expression by ECs. Further, we report that MD-2 facilitates the adhesion of monocytes to ECs by promoting the gene expression of adhesion molecules *CD62E*, *CD54* and *CD106* on ECs. Blocking of CD54 abolished MD-2-induced adhesion of monocytes on ECs indicating that MD-2 is involved



in monocyte recruitment to endothelial cells and progression of systemic inflammation.

Since the presence of macrophages in EMB specimens has previously been shown to be associated with the outcome in DCM patients [37, 38], we determined the influence of MD-2 on monocyte adhesion and activation in *LY96* KO mice. Our data showed a reduced LPS-mediated gene and protein expression of adhesion molecules and NF- $\kappa$ B phosphorylation in *LY96*-KO mice compared to WT mice. Both, enhanced adhesion molecule expression and NF- $\kappa$ B phosphorylation are involved in monocyte adhesion and infiltration [39] emphasizing a role of MD-2 in the adhesion and activation of monocytes.

In summary, our data suggest that MD-2 plays a role in monocyte activation and inflammatory status of patients with DCM. MD-2 does not only act as a LPS-dependent TLR4 co-receptor in the disease process but also act as a soluble biomolecule that stimulates pro-inflammatory processes in macrophages and activates the endothelium facilitating the recruitment and adhesion of monocytes. We propose that MD-2 is a promising therapeutic target to treat disease progression in DCM.

#### AUTHOR CONTRIBUTIONS

RF drafted the article. RF, AK, KL, SG, LL, DL, BC and AS carried out the data collection, analysis and data interpretation and helped writing the manuscript. RF, SF, JF, DL, AR, DW and MD performed study conception and design. JF, DW, DL and SF acquired the funding. All listed authors commented on previous versions of the manuscript and approved the final version of the manuscript.

#### ACKNOWLEDGEMENTS

Graphical abstract was created with [BioRender.com](https://www.biorender.com)

Open Access funding enabled and organized by Projekt DEAL.

#### FUNDING INFORMATION

This work was supported by the European Regional Development Fund (EFRE), the German Technologie-Beratungs-Institut (TBI) (funding code: TBI-V-1-025-VBW-010), the Deutsche Forschungsgemeinschaft (DFG, German Research Foundation (FI 965/5-2 to [JF])), the DZHK (German Center for Cardiovascular Research), partner site Greifswald, (81X2400109 to [SF] and 81Z5400153 to [JF]).

#### CONFLICT OF INTEREST

The authors declare that they have no relationships or conflicts to disclose.

#### DATA AVAILABILITY STATEMENT

The data that supports the findings of this study are available in the supplementary material of this article.

#### CONSENT TO PARTICIPATE

All participants gave written informed consent.

#### CONSENT FOR PUBLICATION

All participants gave written informed consent.

#### PERMISSION TO REPRODUCE

N/A

#### ORCID

Rico Feldtmann  <https://orcid.org/0000-0002-5508-1771>

#### REFERENCES

1. Frantz S, Falcao-Pires I, Balligand J-L, Bauersachs J, Brutsaert D, Ciccarelli M, et al. The innate immune system in chronic cardiomyopathy: a European Society of Cardiology (ESC) scientific statement from the working group on myocardial function of the ESC. *Eur J Heart Fail.* 2018;20(3):445–59.
2. Riad A, Meyer zu Schwabedissen H, Weitmann K, Herda LR, Dorr M, Empen K, et al. Variants of toll-like receptor 4 predict cardiac recovery in patients with dilated cardiomyopathy. *J Biol Chem.* 2012;287(32):27236–43.
3. Yang Y, Lv J, Jiang S, Ma Z, Wang D, Hu W, et al. The emerging role of toll-like receptor 4 in myocardial inflammation. *Cell Death Dis.* 2016;7:e2234.
4. Nagai Y, Akashi S, Nagafuku M, Ogata M, Iwakura Y, Akira S, et al. Essential role of MD-2 in LPS responsiveness and TLR4 distribution. *Nat Immunol.* 2002;3(7):667–72.
5. Sumneang N, Apaijai N, Chattipakorn SC, Chattipakorn N. Myeloid differentiation factor 2 in the heart: bench to bedside evidence for potential clinical benefits? *Pharmacol Res.* 2021; 163:105239.
6. Kim SJ, Kim HM. Dynamic lipopolysaccharide transfer cascade to TLR4/MD2 complex via LBP and CD14. *BMB Rep.* 2017;50(2):55–7.
7. Yu L, Feng Z. The role of toll-like receptor signaling in the progression of heart failure. *Mediators Inflamm.* 2018;2018: 9874109–11.
8. Kaczorowski DJ, Nakao A, McCurry KR, Billiar TR. Toll-like receptors and myocardial ischemia/reperfusion, inflammation, and injury. *Curr Cardiol Rev.* 2009;5(3):196–202.
9. Ciesielska A, Matyjek M, Kwiatkowska K. TLR4 and CD14 trafficking and its influence on LPS-induced pro-inflammatory signaling. *Cell Mol Life Sci.* 2021;78(4):1233–61.
10. Metra M, Teerlink JR. Heart failure. *Lancet.* 2017;390(10106): 1981–95.
11. Yang H, Wang H, Andersson U. Targeting inflammation driven by HMGB1. *Front Immunol.* 2020;11:484.
12. Pugin J, Stern-Voefferay S, Daubeuf B, Matthay MA, Elson G, Dunn-Siegrist I. Soluble MD-2 activity in plasma from patients with severe sepsis and septic shock. *Blood.* 2004;104(13):4071–9.
13. Riad A, Gross S, Witte J, Feldtmann R, Wagner KB, Reinke Y, et al. MD-2 is a new predictive biomarker in dilated cardiomyopathy and exerts direct effects in isolated cardiomyocytes. *Int J Cardiol.* 2018;270:278–86.
14. Wrigley BJ, Lip GYH, Shantsila E. The role of monocytes and inflammation in the pathophysiology of heart failure. *Eur J Heart Fail.* 2011;13(11):1161–71.



15. McNamara DM, Starling RC, Cooper LT, Boehmer JP, Mather PJ, Janosko KM, et al. Clinical and demographic predictors of outcomes in recent onset dilated cardiomyopathy: results of the IMAC (intervention in myocarditis and acute cardiomyopathy)-2 study. *J Am Coll Cardiol*. 2011;58(11):1112–8.
16. Henry WL, Gardin JM, Ware JH. Echocardiographic measurements in normal subjects from infancy to old age. *Circulation*. 1980;62(5):1054–61.
17. Ponikowski P, Voors AA, Anker SD, Bueno H, Cleland JGF, Coats AJS, et al. 2016 ESC guidelines for the diagnosis and treatment of acute and chronic heart failure: the task force for the diagnosis and treatment of acute and chronic heart failure of the European Society of Cardiology (ESC) developed with the special contribution of the heart failure association (HFA) of the ESC. *Eur Heart J*. 2016;37(27):2129–200.
18. Rickham PP. Human experimentation. Code of ethics of the world medical association. Declaration of Helsinki. *Br Med J* 1964;2(5402):177, 1665.
19. Han J, Zou C, Mei L, Zhang Y, Qian Y, You S, et al. MD2 mediates angiotensin II-induced cardiac inflammation and remodeling via directly binding to Ang II and activating TLR4/NF-kappaB signaling pathway. *Basic Res Cardiol*. 2017; 112(1):9.
20. Zegeye MM, Lindkvist M, Fälker K, Kumawat AK, Paramel G, Grenegård M, et al. Activation of the JAK/STAT3 and PI3K/AKT pathways are crucial for IL-6 trans-signaling-mediated pro-inflammatory response in human vascular endothelial cells. *Cell Commun Signal*. 2018;16(1):55.
21. Palsson-McDermott EM, O'Neill LA. Signal transduction by the lipopolysaccharide receptor, toll-like receptor-4. *Immunology*. 2004;113(2):153–62.
22. Fang Q, Wang J, Zhang Y, Wang L, Li W, Han J, et al. Inhibition of myeloid differentiation factor-2 attenuates obesity-induced cardiomyopathy and fibrosis. *Biochim Biophys Acta Mol Basis Dis*. 2018;1864(1):252–62.
23. Zhang Y, Chen H, Zhang W, Cai Y, Shan P, Wu D, et al. Arachidonic acid inhibits inflammatory responses by binding to myeloid differentiation factor-2 (MD2) and preventing MD2/toll-like receptor 4 signaling activation. *Biochim Biophys Acta Mol Basis Dis*. 2020;1866(5):165683.
24. Tissières P, Dunn-Siegrist I, Schäppi M, Elson G, Comte R, Nobre V, et al. Soluble MD-2 is an acute-phase protein and an opsonin for gram-negative bacteria. *Blood*. 2008;111(4):2122–31.
25. Trøseid M, Lind A, Nowak P, Barqasho B, Heger B, Lygren I, et al. Circulating levels of HMGB1 are correlated strongly with MD2 in HIV-infection: possible implication for TLR4-signalling and chronic immune activation. *Innate Immun*. 2013;19(3):290–7.
26. Wrigley BJ, Shantsila E, Tapp LD, Lip GY. CD14++CD16+ monocytes in patients with acute ischaemic heart failure. *Eur J Clin Invest*. 2013;43(2):121–30.
27. Amir O, Spivak I, Lavi I, Rahat MA. Changes in the monocytic subsets CD14(dim)CD16(+) and CD14(++)CD16(–) in chronic systolic heart failure patients. *Mediators Inflamm* 2012;616384-, 2012, 1, 9.
28. Ward JR, Francis SE, Marsden L, Suddason T, Lord GM, Dower SK, et al. A central role for monocytes in toll-like receptor-mediated activation of the vasculature. *Immunology*. 2009;128(1):58–68.
29. Bartekova M, Radosinska J, Jelemensky M, Dhalla NS. Role of cytokines and inflammation in heart function during health and disease. *Heart Fail Rev*. 2018;23(5):733–58.
30. Ueland T, Gullestad L, Nymo SH, Yndestad A, Aukrust P, Askevold ET. Inflammatory cytokines as biomarkers in heart failure. *Clin Chim Acta*. 2015;443:71–7.
31. Kanda T, McManus JE, Nagai R, Imai S, Suzuki T, Yang D, et al. Modification of viral myocarditis in mice by interleukin-6. *Circ Res*. 1996;78(5):848–56.
32. Fontes JA, Rose NR, Čiháková D. The varying faces of IL-6: from cardiac protection to cardiac failure. *Cytokine*. 2015; 74(1):62–8.
33. Park BS, Song DH, Kim HM, Choi B-S, Lee H, Lee J-O. The structural basis of lipopolysaccharide recognition by the TLR4–MD-2 complex. *Nature*. 2009;458(7242): 1191–5.
34. Kevil CG, Patel RP, Bullard DC. Essential role of ICAM-1 in mediating monocyte adhesion to aortic endothelial cells. *Am J Physiol Cell Physiol*. 2001;281(5):C1442–7.
35. Deshmane SL, Kremlev S, Amini S, Sawaya BE. Monocyte chemoattractant protein-1 (MCP-1): an overview. *J Interferon Cytokine Res*. 2009;29(6):313–26.
36. Lehmann MH, Kühnert H, Müller S, Sigusch HH. Monocyte chemoattractant protein 1 (MCP-1) gene expression in dilated cardiomyopathy. *Cytokine*. 1998;10(10):739–46.
37. Nakayama T, Sugano Y, Yokokawa T, Nagai T, Matsuyama TA, Ohta-Ogo K, et al. Clinical impact of the presence of macrophages in endomyocardial biopsies of patients with dilated cardiomyopathy. *Eur J Heart Fail*. 2017;19(4):490–8.
38. Kindermann I, Kindermann M, Kandolf R, Klingel K, Bultmann B, Muller T, et al. Predictors of outcome in patients with suspected myocarditis. *Circulation*. 2008;118(6):639–48.
39. Soetikno V, Sari FR, Veeraveedu PT, Thandavarayan RA, Harima M, Sukumaran V, et al. Curcumin ameliorates macrophage infiltration by inhibiting NF-κB activation and proinflammatory cytokines in streptozotocin induced-diabetic nephropathy. *Nutr Metab*. 2011;8(1):35.

## SUPPORTING INFORMATION

Additional supporting information may be found in the online version of the article at the publisher's website.

**How to cite this article:** Feldtmann R, Kümmel A, Chamling B, Strohbach A, Lehnert K, Gross S, et al. Myeloid differentiation factor-2 activates monocytes in patients with dilated cardiomyopathy. *Immunology*. 2022;167(1):40–53. <https://doi.org/10.1111/imm.13490>